presence of specific ions, the strong adsorption of NO_3^- ion by sulfate precipitates suggests that mixed crystals possibly are formed with nitrate ion superimposed on the primary $BaSO_4$ lattice. This would allow a larger crystal (and consequently a smaller $\sqrt{K_{ss}/K_{SP}}$ for equilibrium) to be formed for a given sized MSO_4 skeleton. If the cation were also strongly adsorbed this tendency would be even more pronounced. The Paneth–Fajans rule of adsorption predicts no change in adsorbing tendency between K^+ and Mg^{++} and no change was found when $Mg(NO_3)_2$ was substituted for KNO_3 in the case of the precipitation of $SrSO_4$. Sr^{++} is predicted to be much more strongly adsorbed than Mg^{++} or K^+ and $Sr(NO_3)_2$. When substituted for $Mg(NO_3)_2$ in the precipitation of $BaSO_4$, it showed a larger decrease in the ratio at the same ionic strength. The effects of solubility and temperature on the observed supersaturation ratio are opposite to one another. Since the higher the solubility the larger is the concentration of ions, that is, in the supersaturated region, the larger is the possible size of any aggregate of ion pairs formed by collisions. This leads to a smaller ratio being required before the aggregate and supersaturation ratio are compatible. The more soluble sulfates of Sr^{++} and Pb^{++} showed a considerably lower supersaturation ratio at their precipitation point.

The increase in the supersaturation ratio with the decrease in temperature, in the case of $BaSO_4$, could well reflect the decrease in the number of collisions per unit concentration which in turn would require a larger concentration of ion pairs to form a given size nucleus.

Summary and Conclusions

1. The maximum limiting concentrations of sulfate ion that can coexist in aqueous solution with barium and strontium ions, respectively, without producing rapid visible precipitation detectable by Tyndall beam, have been investigated for a variety of conditions.

2. To avoid the possibility of local inhomogeneities in concentration as a result of the direct mixing of reagents leading to premature nucleation, sulfate has been generated homogeneously by chemical reactions in the presence of the cations.

3. The data are interpreted in terms of the ratio of the observed mean ion product at the limiting supersaturation $\sqrt{K_{ss}}$ to the corresponding value $\sqrt{K_{SP}}$ at saturation in respect to the stable crystalline phase; *i.e.*, to $\sqrt{K_{ss}/K_{SP}}$. These ratios are sensitive to ionic environment and consequently require correction to unit values of the activity coefficient, namely, to $\sqrt{K^0_{ss}/K^0_{SP}}$, the mean activity product ratio.

4. The uncorrected ratio for barium sulfate varies from 55 to 48; when corrected to unit activity coefficient, assuming the activity coefficient of barium sulfate behaves like that of zinc and cadmium sulfates, the ratio assumes a constant value of 21.5. This corrected ratio now varies little if at all with ionic strength except on the addition of specific foreign neutral salts. The ratio decreases with rising temperature.

5. The technique of direct mixing of reagents gives limiting supersaturation values which decrease uniformly with the elapsed time required for the appearance of the Tyndall beam. When extrapolated to an elapsed time of zero, the corrected ratio becomes 21.2 in excellent agreement with the preceding result.

6. The corrected ratio for strontium sulfate is 2.9.

7. The results of Von Weimarn when recalculated to unit activity coefficient become consistent with our values.

8. The problem of nucleation is discussed in the light of modern theories of phase transitions.

NEW YORK, N. Y. RECEIVED JULY 10, 1950

[CONTRIBUTION FROM THE INSTITUTE FOR THE STUDY OF METALS, UNIVERSITY OF CHICAGO]

A Thermodynamic Study of Liquid Metallic Solutions. III. The Systems Bismuth–Gold and Thallium–Gold

BY O. J. KLEPPA*

In earlier communications dealing with the liquid systems lead–gold[1] and tin–gold[2] the author has pointed out the importance of gathering further information on liquid metallic mixtures. As in the earlier investigations the electromotive force method was used to obtain information on the chemical potentials and partial molal entropies of the binary solutions. In the two systems under investigation the reversible galvanic cells take the form

$$\mathrm{Bi(l)/Bi^{+++}/(Bi + Au)(l)}$$

and

$$\mathrm{Tl(l)/Tl^{+}/(Tl + Au)(l)}$$

Series of alloys containing from zero to about 80 atomic per cent. gold were investigated at temperatures from about 400° up to more than 800° for alloys rich in gold.

Experimental Procedure

(A) General.—The experimental procedure was analogous to the one used in the case of the system tin-gold,[2] with the following modifications.

In order to study alloys containing more than 55–60 atomic per cent. gold, a closed type silica or vycor cell was devised which could be used above 630°, the upper limit for use of Pyrex cells. Because of the impossibility of making gas-tight tungsten–silica and tungsten–vycor seals, the following two alterations of the closed type cell were used.

Type 1 cell (Fig. 1(a)) was made from silica or vycor tubing of 9–10 mm. o.d., and was fitted with two Pyrex-

---

* Norwegian Defense Research Establishment, Lillestrøm, Norway.

[1] O. J. Kleppa, THIS JOURNAL, **71**, 3275 (1949).

[2] O. J. Kleppa, *ibid.*, **72**, 3346 (1950).

silica graded seals in order to allow a gas-tight seal of tungsten to Pyrex outside the hottest region of the furnace. The cell was charged through the two side tubes, which could later be sealed off. A small hole in the capillary which protected the tungsten wire served to equalize the pressure.

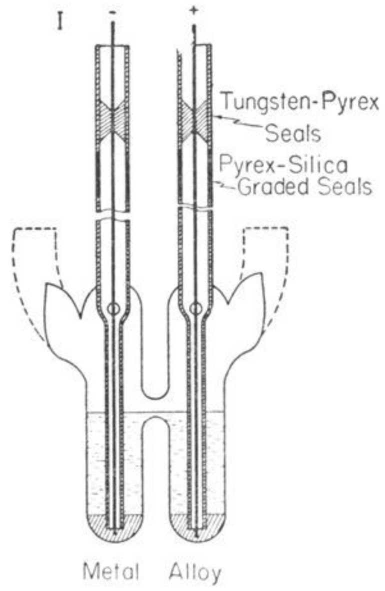

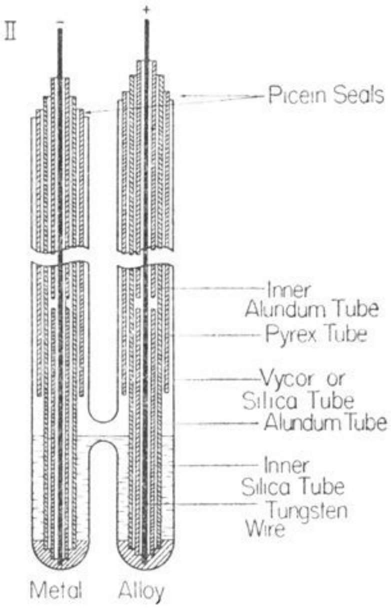

Figs. 1(a) and 1(b).—Closed type cells made from silica or vycor glass for use above 630°.

Fig. 1(b).

Type 2 cell (Fig. 1(b)) consisted of an outer H-shaped cell made of silica or vycor tubing, and of sufficient length to extend well out of the furnace. The tungsten leads were fitted with concentric silica, alundum and Pyrex tubes in order to protect the leads in the gas phase and in the electrolyte melt and to reduce the "dead space" of the cell. The cell was charged from the top and sealed with picein.

Both types of cell were found to be reasonably satisfactory, although type 2 provided better protection of the tungsten leads from the highly corrosive chloride vapors inside the cell. For prolonged runs cell type 2 was therefore the more satisfactory. At temperatures above 800° the cell walls deteriorated rapidly, a fact which reduced the useful cell life to 24 hours or less.

The actual operational procedure was analogous to that used in the case of tin–gold, with the obvious exception that the electrolyte now contained a few (3–5) weight per cent. of $BiCl_3$ or TlCl instead of $SnCl_2$.

As before, after completion of each run the pure metal reference electrodes were checked for the presence of gold by spectrographic means. In all the reported cases for the bismuth–gold runs less than 0.03% Au was found, while the corresponding figure for the thallium–gold runs was 0.007% Au.

The bismuth and thallium were subjected to spectrographic analysis and the presence of the following impurities detected.

Metal	Impurity	Amount, %
Bi	Mg, Al, Ag, Si	~0.01
	Cu, Pb	~ .001
Tl	Mg, Ca, Si, In	~ .01
	Al, Cu, Pb	~ .001

The gold was the same "fine gold" used for the earlier investigations.

(B) Bismuth–Gold Alloys.—In the case of these alloys it was found that the electromotive force was more sensitive to temperature fluctuations than it had been in the earlier investigations. While, for example, reproducible results in those cases were obtained even during periods of slight drift in temperature, this was now no longer true. This difference is believed to be due, at least in part, to the volatility of $BiCl_3$ (b.p. 447°), which may facilitate the formation of local gradients in the concentration of Bi^{+++} ions in the electrolyte during changes in temperature.

For experiments carried out in all-Pyrex cells at 450–630° the reproducibility was, however, still good, generally better than ±0.05 mv. The precision dropped gradually at the higher temperatures. As found during investigation of the system lead–gold, the practical upper limit in temperature seemed to be 800–850°, and the results reported below for this temperature region are associated with a possible error of about ±0.5 mv. (about 1% of the electromotive force). Errors even of this magnitude are not too serious in the calculation of chemical potentials and activities. However, in order to obtain partial molal entropies, the temperature coefficient of the electromotive force must be established and the entropy data for the gold-rich solutions are therefore somewhat uncertain. This will be noticed in the increased scattering of points in Fig. 2.

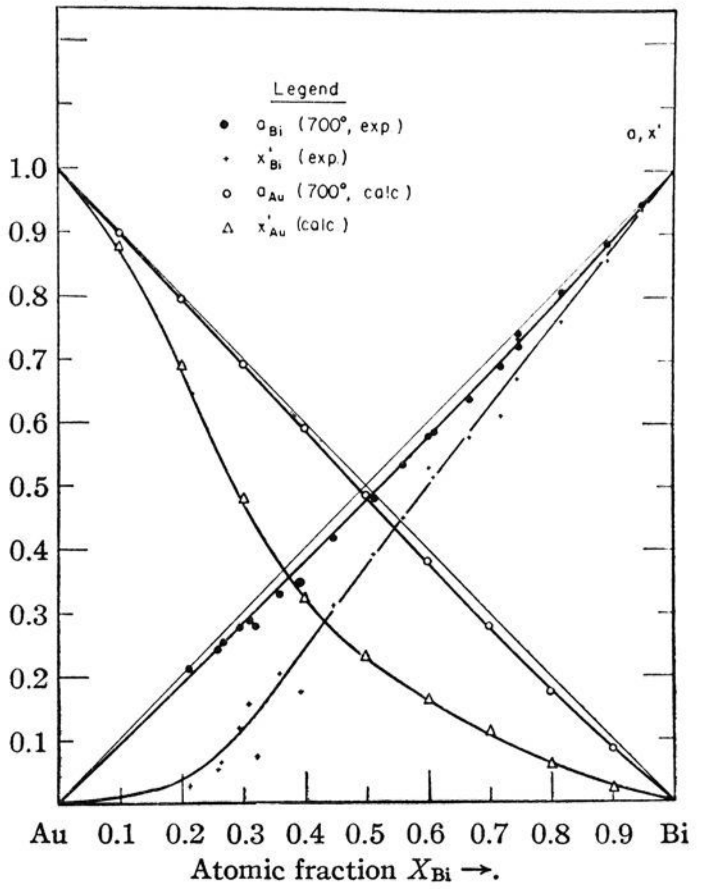

Fig. 2.—Activities and "Entropy Fractions" in the system Bi(l)–Au(l).

During one of the first runs at the higher temperatures a slight drift in the measured electromotive force with time was detected over a period of about one day. It was suspected that this drift might be due to transfer of gold from the alloy side to the pure metal side of the cell, a suspicion which was confirmed by the subsequent chemical analysis. The reference electrode in this particular case showed 0.3% gold after completion of the run.

The mechanism of this transfer reaction is unclear, as AuCl and $AuCl_3$ should be unstable at those high temperatures, and gold could not be detected spectrographically in the electrolyte after completion of the run. It was possible, however, to suppress the drift in the electromotive force and the transfer reaction by using as a reference electrode an alloy containing 80–90 atomic per cent. of bismuth, the remainder being gold.

The composition of the alloy electrodes after completion of the run was determined by chemical analysis. No change in composition was found within the error of the analytical method.

(C) Thallium–Gold Alloys.—The first runs in this alloy system showed a slight increase in electromotive force with time. This was found to be due to loss of metallic thallium from the alloy present in the cell. Such a loss had not been observed in the previously investigated systems, which involved the more "noble" metals, tin, lead and bismuth. It was found that the loss of metal was due to oxidation by traces of water present in the electrolyte melt. This difficulty was overcome by carrying out the later runs with an electrolyte which had been treated in the molten state with metallic sodium prior to the run. In these cases no drift, or at most a drift of the order of a few hundredths of a millivolt, was observed, and chemical analysis of the alloys after completion of the run showed no change in composition within the error of the analytical method. The alloy compositions obtained by the final chemical analysis of the alloy are reported below.

With the use of the sodium-treated salt melt the precision and reproducibility of the electromotive force measurements in this system, when carried out in Pyrex cells at moderate temperatures, became comparable to what was obtained in the system lead–gold and tin–gold. At higher temperatures the precision dropped, and, as in the other cases reported, 800–850° was found to be the practical upper limit in temperature.

Experimental Results

The treatment of the experimental results and the determination of the temperature gradients of the electromotive force were carried out as before. In order to avoid the rather long extrapolation of the more uncertain high temperature data to the common reference temperature of 600° (used in the earlier investigations), it was decided to refer all data to the common reference temperature of 700°. This involved extrapolation also of the data obtained in Pyrex cells at 450–630°.

In Table I(a) are summarized the experimental results of a total of 20 runs on bismuth–gold alloys, as well as activities and "entropy fractions"[1] for bismuth computed from these data. In order to arrive at activities and "entropy fractions" for the cases where the reference electrode was an alloy, use was made of the data—already obtained—for alloys low in gold. Similarly in Table I(b) are given the experimental results for 13 runs on thallium–gold alloys. Based on these sets of experimental data, the activities and "entropy fractions" for bismuth and thallium at round figure atomic fractions were determined by graphical interpolation of the smooth curve drawn through the experimental points. These quantities appear in the second and fourth columns of Tables II(a) and II(b). From these data the corresponding activities and "entropy fractions" for gold in the solutions were calculated by graphical integration. These data will be found in columns 3 and 5 of the same tables. Finally, the relative partial molal heat contents and the integral heats of mixing, $\overline{L}$ and ΔH, were computed for both systems. These quantities are recorded in the last three columns of the tables.

TABLE I(a)

EXPERIMENTAL RESULTS AND CALCULATED ACTIVITIES AND "ENTROPY FRACTIONS" IN THE SYSTEM AU(l)–BI(l)

Results in parentheses are obtained by extrapolation

Run	Weighed in X_{Bi}	Reference X_{Bi}	E(mv.) at 600°	E(mv.) at 700°	E(mv.) at 800°	$\Delta E/\Delta T$ (mv./100°)	a_{Bi} 700°	X'_{Bi}
1	0.892$_6$	1.000	3.01	(3.4$_5$)	..	0.44	0.88$_4$	0.85$_8$
3	.748$_3$	1.000	7.43	(8.3$_1$)	..	0.88	.74$_3$	.73$_6$
4	.601$_5$	1.000	13.43	(15.2$_6$)	..	1.83	.57$_9$	.52$_9$
5	.512$_5$	1.000	17.88	(20.5$_6$)	..	2.68	.47$_9$	.39$_3$
6	.948$_0$	1.000	1.38	(1.5$_6$)	..	0.18	.94$_6$	.93$_9$
7	.818$_7$	1.000	5.18	(5.9$_6$)	..	.78	.80$_8$	.76$_2$
8	.719$_8$	1.000	8.98	(10.3$_8$)	..	1.4$_0$	.69$_0$	.61$_4$
10	.447$_5$	1.000	21.15	(24.5$_0$)	..	3.3$_5$	.41$_6$	.31$_1$
11	.319$_2$	1.000	...	35.$_7$	..	7.5	.27$_9$	.07$_3$
12	.561$_5$	1.000	15.20	(17.5$_0$)	..	2.3$_0$	.53$_5$	.44$_9$
13	.609$_7$	1.000	13.01	(14.9$_2$)	..	1.91	.58$_6$	.51$_4$
14	.391$_5$	1.000	24.6	29.$_6$	..	5.$_0$	.34$_7$	.17$_5$
15	.669$_0$	1.000	10.96	(12.5$_4$)	..	1.5$_8$	.63$_8$	.57$_7$
16	.747$_8$	1.000	7.90	(9.0$_5$)	..	1.1$_5$	.72$_3$	.67$_0$
17	.293$_5$	0.801$_0$	...	29.$_3$	34.$_6$	5.$_3$	.27$_7$	.11$_8$
18	.358$_9$	.903$_6$	...	28.$_1$	..	4.$_2$	.32$_9$	.20$_3$
19	.258$_6$	.799$_2$	...	(33.$_1$)	40.$_7$	7.$_6$	.24$_2$	.05$_8$
20	.309$_7$	.8947	...	31.$_7$	..	4.$_9$	.28$_6$	.15$_7$
21	.267$_4$	.896$_4$	...	(35.$_0$)	42.$_5$	7.$_5$	.25$_4$	.06$_4$
22	.212$_5$	.898$_5$	...	(40.$_2$)	50.$_2$	10	.21$_2$	.02$_7$

TABLE I(b)

EXPERIMENTAL RESULTS AND CALCULATED ACTIVITIES AND "ENTROPY FRACTIONS" IN THE SYSTEM AU(l)–Tl(l)

Results in parentheses are obtained by extrapolation

Run	Composition X_{Tl}	E(mv.) at 600°	E(mv.) at 700°	E(mv.) at 800°	$\Delta E/\Delta T$ (mv./100°)	a_{Tl} 700°	X'_{Tl}
1	0.895	9.15	(10.3$_2$)	...	1.1$_7$	0.88$_4$	0.87$_3$
2	.794	20.50	(22.9$_5$)	...	2.4$_5$	.76$_1$	.75$_3$
3	.681	37.85	(42.3$_5$)	...	3.5$_0$	.60$_3$	.59$_3$
4	.587	54.60	(61.0)	...	6.4$_0$	.48$_3$	.47$_6$
5	.485	48.80	(88.3)	...	9.5$_0$	.34$_9$	.33$_2$
6	.382	104.2	(116.$_2$)	...	12.$_0$	.25$_0$	.24$_8$
7	.421	93.35	(104.4$_5$)	...	11.$_1$	.28$_8$	.27$_6$
8	.595	53.80	(59.9$_0$)	...	6.1$_0$	.49$_1$	.49$_3$
9	.405	101.25	(113.$_2$)	...	12.$_0$	.26$_0$	.24$_8$
13	.535	67.15	(74.9$_5$)	...	7.8$_0$	.40$_9$	.40$_4$
14	.337	....	131.$_5$	...	13.$_5$	.20$_8$	.20$_8$
16	.243	....	(169.$_6$)	187.$_2$	17.$_6$	.13$_2$	.13$_0$
17	.17$_7$	....	(199)	(220)	21	.09$_3$	.08$_7$

In Fig. 2 will be found plots of the experimental and computed activities and "entropy fractions" for the system bismuth–gold, and in Fig. 3 are plotted the same data for thallium–gold. Finally will be found in Figs. 4 and 5 the thermal data for the two systems.

TABLE II(a)

COMPUTED THERMODYNAMIC DATA FOR THE SYSTEM AU(l)–BI(l)

The reference state for gold is the hypothetical undercooled liquid gold. Figures in parentheses are based on extrapolation.

X_{Bi}	a_{Bi} 700°	a_{Au} 700°	X'_{Bi}	X'_{Au}	$\overline{L}_{Bi}$, cal.	$\overline{L}_{Au}$, cal.	ΔH, cal.
1.000	1.000	0.000	1.000	0.000	0	(2500)	0
0.900	0.89$_4$	.08$_4$	0.87$_5$	.02$_5$	40	2350	270
.800	.79$_0$	.17$_6$	.74$_5$	.06	110	2050	500
.700	.68$_0$	.27$_8$	.62$_0$	.11	180	1850	680
.600	.57$_5$	.38$_0$	.50$_0$	.16	270	1690	840
.500	.47$_0$	.48$_6$	.37$_5$	.23	440	1460	950
.400	.37$_0$	.59$_2$	.24$_5$	.32	800	1170	1020
.300	.27$_5$	.69$_5$	.12$_0$	.48	1600	730	990
.200	.18$_5$	.79$_7$	.04	.69	2960	280	820
.100	(.09)	.89$_9$	(.01)	.88	(4250)	50	470
.000	.000	1.000	.000	1.000	(5500)	0	0

TABLE II(b)

COMPUTED THERMODYNAMIC DATA FOR THE SYSTEM AU(l)–Tl(l)

The reference state for gold is the hypothetical undercooled liquid gold. Figures in parentheses are based on extrapolation.

X_{Tl}	a_{Tl} 700°	a_{Au} 700°	X'_{Tl}	X'_{Au}	$\overline{L}_{Tl}$, cal.	$\overline{L}_{Au}$ cal.	ΔH, cal.
1.000	1.000	0.000	1.000	0.000	0	(150)	0
0.900	0.88$_9$	.04$_0$	0.88$_2$	.03$_8$	16	120	26
.800	.76$_5$	.10$_2$	.75$_6$	.09$_6$	20	86	33
.700	.63$_0$	.18$_1$	.62$_1$	.17$_6$	28	62	38
.600	.49$_5$	.28$_6$	.48$_6$	.27$_8$	36	48	40
.500	.37$_2$	.40$_5$	.36$_3$	.40$_0$	53	26	40
.400	.26$_6$	.53$_5$	.25$_6$	.53$_3$	74	8	34
.300	.17$_7$	.66$_6$	.17$_0$	.66$_5$	84	2	27
.200	.10$_6$	.79$_0$	.10$_2$	.78$_7$	74	5	19
.100	(.05$_0$)	.89$_7$	(.04$_7$)	.89$_6$	103	1	11
.000	.000	1.000	.000	1.000	(115)	0	0

Activity of Gold from Phase Diagram

According to Hansen[3] the equilibrium phase diagrams for the two systems bismuth–gold and thallium–gold are very similar, showing in the main a simple eutectic behavior, with very limited solid solubilities of bismuth and thallium in gold.

We should accordingly be able to compute the

---

(3) M. Hansen, "Aufbau der Zweistofflegierungen," Berlin, 1936.

activities of gold in the liquid solutions with respect to the hypothetical, undercooled liquid gold in the manner outlined in the paper on lead–gold.[1] Based on the two simple assumptions (a) $\Delta C_P = 0$ for the process Au(l) = Au(s) and (b) negligible solid solubility of the more electropositive metal in gold, a formula was derived for the activity of gold in the liquid solutions along the "liquidus"

$$\log a_{\mathrm{Au}} = 0.4957 - 662.3/T$$

where T is the temperature in °K.

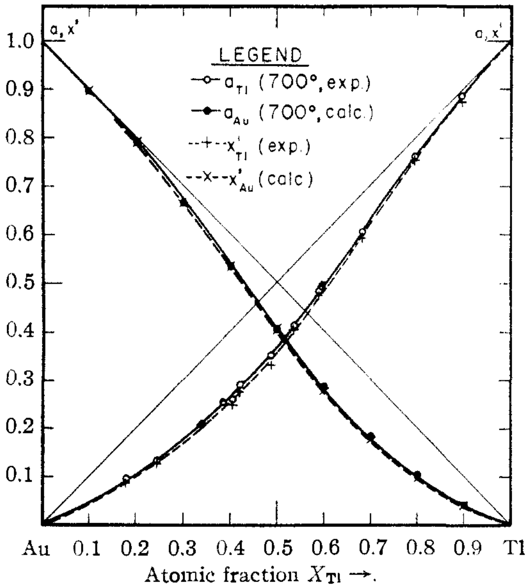

Fig. 3.—Activities and "Entropy Fractions" in the system Tl(l)–Au(l).

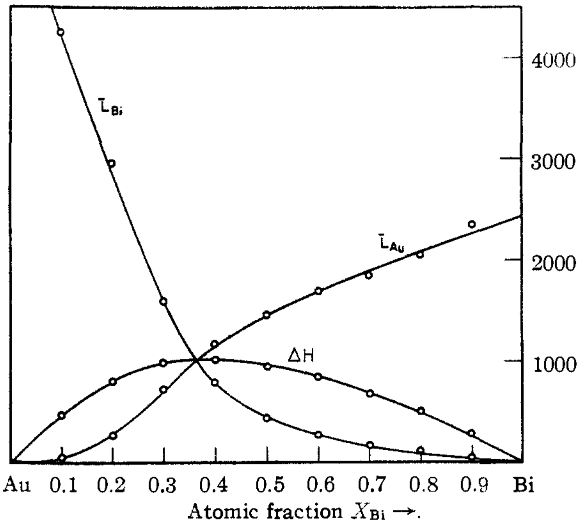

Fig. 4.—Relative partial molal heat contents, and integral heats of mixing in the system Bi(l)–Au(l).

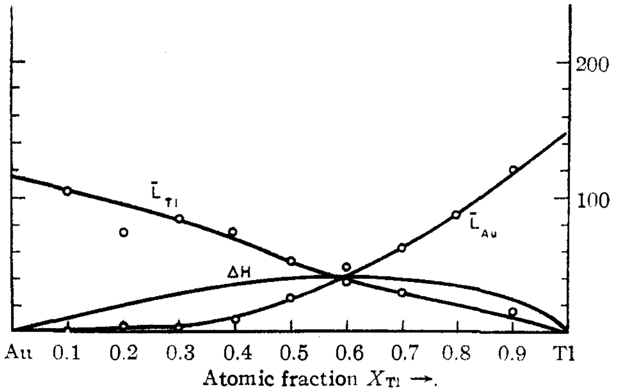

Fig. 5.—Relative partial molal heat contents, and integral heats of mixing in the system Tl(l)–Au(l).

We have referred the measurements in the present case to the common reference temperature of 700°, and find by using this formula

$$a_{\mathrm{Au}}\ (700°) = 0.65_5$$

By consulting the phase diagrams we find for the compositions at the "liquidus" corresponding to this temperature $X_{\mathrm{Bi}} = 0.32$ and $X_{\mathrm{Tl}} = 0.31$, respectively. From Figs. 2 and 3 we find that the corresponding activities of gold are 0.67_5 (Au–Bi) and 0.65_5 (Au–Tl).

The agreement in the case of the system thallium–gold is better than should be expected, since Levin,[4] who investigated this system, states that his liquidus curve may be associated with an error of about 10°, which corresponds to an uncertainty of about 1% in composition or activity.

The discrepancy in the case of the bismuth–gold system becomes less significant if we assume a similar uncertainty in the accepted phase diagram for this system. It is known, for example that the bismuth metal used by Vogel in the investigation of this system[5] had a melting point of 266°, while the accepted value is 271°. It is, however, also quite possible that some of the discrepancy originates in our extrapolation of the most uncertain data for bismuth into the very gold-rich solutions. In fact, a possible way of calculating from our data the activities of gold in the solutions less rich in gold would have been to accept the value obtained from the phase diagram as the starting point and carry on from there as before by means of the Gibbs–Duhem equation.

In the case of the system thallium–gold, the results of the present investigation indicate that the phase diagram may be used for comparison with our results even for other compositions and temperatures than the ones used above. This is due to the fact that the heat of mixing in this particular system was found to be very small ($\Delta H < 50$ cal., $\bar{L} \lesssim 100$ cal.), and may accordingly be neglected without introducing any very serious error. It follows that the activities determined above for the common reference temperature of 700° may be considered with good approximation to be correct also for other temperatures. It should thus be permissible to calculate activities for gold from the phase diagram for a wide range of temperatures and compositions and compare them with our experimental results at 700°. We have presented in Table III the results of this comparison.

The excellent agreement obtained in this comparison must be considered as substantial evi-

---

[4] M. Levin, *Z. anorg. allgem. Chem.*, **45**, 31 (1905).

[5] R. Vogel, *ibid.*, **50**, 145 (1906).

TABLE III

ACTIVITIES OF GOLD FROM THE PHASE DIAGRAM AT VARIOUS TEMPERATURES COMPARED WITH ACTIVITIES AT 700° OBTAINED IN THE PRESENT WORK

The reference state is the hypothetical, undercooled liquid gold.

Compn. X_{Au}	Liquidus °K.	a_{Au} ph. diagr.[a]	a_{Au} 700°, pres. work
1.00	1336 (m.p.)	1.00	1.00
0.90	1225	0.901	0.897
.80	1105	.787	.790
.70	985	.666	.666
.60	860	.532	.535
.50	725	.382	.405

[a] From log a = 0.4957 − 662.3/T.

dence for the validity of the assumptions on which the comparison is built.

Discussion

The thermodynamic properties of the liquid systems gold–bismuth and gold–thallium show certain unusual and interesting features which will presently be considered in somewhat more detail.

Let us first focus our attention on an important common feature of the two systems. They both show large positive entropy deviations when compared with the ideal solution (see "entropy fractions," Figs. 2 and 3). The previous papers[1,2] discussed some of the factors affecting the entropy of mixing in binary solutions. In particular, an attempt was made to explain the very large positive entropy deviation which are occasionally found in liquid metallic systems on the basis of vibrational entropy terms, largely originating in the packing problems involved in the mixing of atoms of widely different size. In the case of bismuth–gold and thallium–gold we have new examples of such mixtures involving the small gold atom and the much larger thallium and bismuth atoms. However, the similar features of the two systems do not go beyond the large positive entropy deviation. In the case of the gold–bismuth system the activity data for 700° indicate that the system exhibits only a slight negative deviation from Raoult's law. If the solution had shown an ideal entropy of mixing ("regular solution"), this slight deviation would have meant that the solution was formed with slight evolution of heat, $\Delta H < 0$. Actually, however, the system shows a considerable heat absorption on mixing, with positive values of ΔH of the order of $\sim$1 kcal./g. atom in the middle of the system. The tendency toward positive deviation from Raoult's law is in this case balanced by the already mentioned large positive entropy deviation, which gives the system the appearance of being nearly ideal at 700°. An interesting aspect of this relationship is the unusual phenomenon that the negative deviation from Raoult's law increases with increasing temperature, while at sufficiently low temperatures we should expect positive deviation.

The system thallium–gold shows a very different picture. In this case the heat of mixing is very small ($\Delta H < 50$ cal.), and the large positive entropy deviation predominates. The net result is that the system shows a fairly large negative deviation from Raoult's law. In fact, the nearly identical values found for activity and "entropy fraction" in this system make it extremely difficult to evaluate accurately the actual heat terms involved. The thermal data given in Table III(b) and plotted in Fig. 5 should, therefore, be considered as establishing only the order of magnitude of these heat terms.

The data on partial molal heat contents and integral heats of mixing for the system bismuth–gold presented in Fig. 4 direct our attention to another point of interest. It will be seen from this figure that the relative partial molal heat content for gold in bismuth at high dilution is only about half as large as for bismuth in gold. Accordingly, we find that the maximum in the curve for the heat of mixing is displaced toward the gold-rich side of the system (X_{Au} = 0.63). We shall see presently that it appears generally to be the case that whenever two metals show a marked positive ΔH of mixing, the maximum is displaced toward the side of the *smaller* atom. In Table IV are found values of ΔH available in the literature and obtained from electromotive force measurements of liquid systems which show a *positive* ΔH of mixing. We have also established the composition at which the maximum heat of mixing is found, and recorded the results in the last column. The list could be considerably extended by including the results of calorimetric measurements.

TABLE IV

HEAT OF MIXING FROM ELECTROMOTIVE FORCE MEASUREMENTS IN LIQUID SYSTEMS SHOWING POSITIVE ΔH OF MIXING

System	ΔH max. kcal./g. atom	Compn. of max. X (smaller atom)
Ag–Sn[9]	+1.36	0.52 (Ag)
Au–Bi	1.04	.63 (Au)
Au–Tl	0.04	.45 (Au)
Bi–Cd[6]	.22	.7 (Cd)
Bi–Sn[7]	.02	.50 (Sn)
Cd–Pb[6]	.69	.60 (Cd)
Cd–Sn[6]	.48	.60 (Cd)
Cd–Zn[6]	.53	.48 (Zn)
Sn–Tl[8]	.63	.50 (Sn)
Sn–Zn[6]	.82	.60 (Zn)

It will be seen that the rule is supported by most of the reported data, the only important exceptions here being the systems Au–Tl and Cd–Zn. Additional support for this rule may be found by examination of the phase diagrams of simple binary systems with limited miscibility in the liquid state; for example, Bi–Zn, and Pb–Zn. It will as a rule be found that the segregation is unsymmetrical in composition with a maximum (critical temperature–composition) at concentrations richer in the smaller atom. This lack of symmetry in the segregation loop is of course related to a similar lack of symmetry in the ΔH of mixing. Both the unsymmetrical appearance of the ΔH curves and, to some extent also, the magnitude of ΔH,

---

(6) N. W. Taylor, THIS JOURNAL, 45, 2871 (1923).

(7) Seltz and Dunkerley, *ibid.*, 64, 1393 (1942).

(8) Hildebrand and Sharma, *ibid.*, 51, 462 (1929).

(9) Frantik and McDonald, *Trans. Am. Electrochem. Soc.*, 88, 253 (1945).

may possibly be explained by the difference in atomic volume of the two components.

In an explanation of this asymmetry, the importance of atomic size may arise from its effect on the number of nearest neighbors in the mixture. Thus the larger bismuth atoms, in a matrix primarily of smaller gold atoms, will have a larger number of nearest neighbors than the small gold atoms, in a matrix primarily of larger bismuth atoms. To the author's knowledge, no attempt has been made in the literature to evaluate this effect quantitatively, but it may be assumed to play an important part in the understanding of the energetic asymmetry of binary mixtures.

There is also a fair amount of qualitative support for the idea that the magnitude of ΔH is related to a difference in size between the two components. It is, for example, well known that pairs of metals of widely different atomic size frequently show limited miscibility in the liquid state. It may be mentioned that the same point of view underlies discussions of the size factor in connection with solid solubility.

The effect of size differences on specific heat and, consequently, on heat and entropy of mixing gives further support for the same idea. However, although it is clear that this difference in specific heat should contribute toward the measured positive value of ΔH at elevated temperature, one also has to take into account the hypothetical interaction energy at the absolute zero. We are, at the present time, unable to estimate the relative importance of these two factors.

Acknowledgments.—The author is indebted to Miss M. C. Bachelder, Mr. Adolph Roman and Mr. L. J. Howell for carrying out the analytical work involved in the present investigation.

Summary

The thermodynamic properties of the liquid systems bismuth–gold and thallium–gold have been investigated by the electromotive force method.

Both systems show the expected large entropies of mixing, which are believed to originate in the large differences in atomic size between the two components.

In the system bismuth–gold the combined effect of the entropy and a fairly large positive ΔH of mixing (1 kcal./g. atom in the middle of the system) is to give the system a nearly ideal appearance at 700°. In the thallium–gold system the large entropy terms entirely overshadow the heat terms, causing the system to show fairly large negative deviations from Raoult's law.

Chicago, Illinois Received June 19, 1950

[Contribution from the School of Chemistry of the University of Minnesota]

Reaction of Ferrous and Ferric Iron with 1,10-Phenanthroline. IV. Application to Investigation of Zinc Phenanthroline Complexes

By I. M. Kolthoff, D. L. Leussing and T. S. Lee[1]

Zinc ion has been shown to form three complexes with 1,10-phenanthroline in aqueous solution: the mono-, di- and tri-1,10-phenanthroline zinc ion. The equilibrium constants for these complexes have been evaluated and found to be 3.7×10^{-7}, 7×10^{-13} and 1×10^{-17} for K_1, K_2 and K_3, respectively, at 25°.

Zinc has been observed to interfere in the colorimetric determination of iron by 1,10-phenanthroline,[2] indicating that 1,10-phenanthroline forms one or more relatively strong complexes with zinc. Additional evidence for the existence of zinc–phenanthroline complexes is that solid zinc triphenanthroline[3] and the similar mono- and tridipyridyl complexes have been described in the literature.[4]

The following investigation has been carried out in order to establish the nature and equilibrium constants of the zinc–phenanthroline complexes in aqueous solutions. This investigation also illustrates how knowledge of the complex ions of one metal (ferrous phenanthroline complexes) may be used in the study of the complex ions of another metal.

The dissociation constant of the mono-phenanthroline-zinc ion was evaluated by allowing zinc and ferrous iron to compete for a limited amount of phenanthroline and measuring the equilibrium concentration of triphenanthroline ferrous ion (ferroin) spectrophotometrically. The dissociation constants of the di- and triphenanthroline zinc complexes were evaluated from experiments in which the equilibrium distribution of phenanthroline between chloroform and aqueous zinc solution was determined. In addition, conductometric measurements were made which verify the results obtained by both of the above methods.

Monophenantholine Zinc Ion: Competition Experiments

The molar concentration, *y*, of *o*-phenanthroline present as zinc complexes in a solution containing zinc, ferrous iron and phenanthroline is given by the expression

$$y = C_{\mathrm{Ph}} - 3[\mathrm{FePh_3}^{++}] - [\mathrm{FePh}^{++}] \qquad (1)$$

where C denotes total, analytical concentration brackets represent actual concentrations, and Ph represents the phenanthroline molecule. Under the experimental conditions used the concentration of free phenanthroline can be neglected in equation

---

(1) Department of Chemistry, University of Chicago, Chicago, Illinois.

(2) Smith and Richter, "Phenanthroline and Substituted Phenanthroline Indicators," G. Frederick Smith Chemical Co., Columbus, Ohio; E. B. Sandell, "Colorimetric Determination of Traces of Metals," Interscience Publishers, Inc., New York, N. Y., 1944, p. 271.

(3) F. Blau, *Monatsh.*, **19**, 647 (1898); P. Pfeiffer and Fr. Tapperman, *Z. anorg. allgem. Chem.*, **215**, 273 (1933); P. Pfeiffer and K. Quehl, *Ber.*, **64**, 2667 (1931); **65**, 560 (1932).

(4) F. M. Jeager and J. A. van Dijk, *Z. anorg. allgem. Chem.*, **227**, 273 (1936).